Molecules and Cells

Anastral Spindle 3/Rotatin Stabilizes Sol narae and Promotes Cell Survival in *Drosophila melanogaster*

Dong-Gyu Cho[1], Sang-Soo Lee[1,2], and Kyung-Ok Cho[1,*]

[1]Department of Biological Sciences, Korea Advanced Institute of Science and Technology (KAIST), Daejeon 34141, Korea, [2]Present address: Center for Bioanalysis, Korea Research Institute of Standard and Science, Daejeon 34113, Korea
*Correspondence: kocho@kaist.ac.kr
https://doi.org/10.14348/molcells.2020.0244
www.molcells.org

Apoptosis and compensatory proliferation, two intertwined cellular processes essential for both development and adult homeostasis, are often initiated by the mis-regulation of centrosomal proteins, damaged DNA, and defects in mitosis. Fly Anastral spindle 3 (Ana3) is a member of the pericentriolar matrix proteins and known as a key component of centriolar cohesion and basal body formation. We report here that *ana3*^{m19} is a suppressor of lethality induced by the overexpression of Sol narae (Sona), a metalloprotease in a disintegrin and metalloprotease with thrombospondin motif (ADAMTS) family. *ana3*^{m19} has a nonsense mutation that truncates the highly conserved carboxyl terminal region containing multiple Armadillo repeats. Lethality induced by Sona overexpression was completely rescued by knockdown of Ana3, and the small and malformed wing and hinge phenotype induced by the knockdown of Ana3 was also normalized by Sona overexpression, establishing a mutually positive genetic interaction between *ana3* and *sona*. p35 inhibited apoptosis and rescued the small wing and hinge phenotype induced by knockdown of *ana3*. Furthermore, overexpression of Ana3 increased the survival rate of irradiated flies and reduced the number of dying cells, demonstrating that Ana3 actively promotes cell survival. Knockdown of Ana3 decreased the levels of both intra- and extracellular Sona in wing discs, while overexpression of Ana3 in S2 cells dramatically increased the levels of both cytoplasmic and exosomal Sona due to the stabilization of Sona in the lysosomal degradation pathway. We propose that one of the main functions of Ana3 is to stabilize Sona for cell survival and proliferation.

Keywords: Ana3, apoptosis, Arrow, cell death, exosome, radiation, Rotatin, Sona

INTRODUCTION

The ability to resist and recover from external stresses is important for all living organisms that face stresses such as heat, reactive oxygen species, and irradiation during development and in the adult stage. Damaged cells need to be removed by apoptosis and replaced with newly formed cells by compensatory proliferation. The wing imaginal disc of *Drosophila melanogaster* is the primordium of the adult wing, and shows a very low level of cell death during normal larval development. In contrast, it shows extensive cell death by environmental stresses, and yet can develop into a normal wing even after 40% to 60% cell death (Jaklevic and Su, 2004; Karpen and Schubiger, 1981).

The centrosome consists of a pair of centrioles and pericentriolar materials (PCMs). DNA damage and mitotic defects cause the overduplication of centrosomes and the formation of multipolar spindles, leading to mitotic failure and cell death (Vakifahmetoglu et al., 2008). Defects in PCMs interrupt spindle assembly and activate the spindle assembly checkpoint (Torres et al., 2011). Fly Anastral spindle 3 (Ana3)

Received 10 December, 2020; accepted 16 December, 2020; published online 26 January, 2021

eISSN: 0219-1032

is a PCM responsible for the cohesion of centrioles, prevention of premature centriolar segregation, and formation of basal bodies (Stevens et al., 2009). Ana3 and its mammalian homolog Rotatin (RTTN) contain multiple Armadillo repeats known to interact with Wnt signaling components and potentiate the Wnt pathway (Song et al., 2003). Wnt has critical roles in growth, development, adult homeostasis, and regeneration (Clevers and Nusse, 2012; Logan and Nusse, 2004; Raslan and Yoon, 2020). Ana3 and RTTN are also important for the formation of cilia and basal bodies (Kheradmand Kia et al., 2012; Stevens et al., 2009). Loss of RTTN causes polymicrogyria (PMG), situs inversus, isomerism, and heterotaxia in humans (Vandervore et al., 2019).

From a previous genetic screen, we found 28 mutants as responsible for the suppression of lethality caused by the overexpression of Sol narae (Sona) (Kim and Cho, 2020). In the present work, we identified one of suppressors as *ana3*^{m19}. Sona is a member of a disintegrin and metalloprotease with thrombospondin motif (ADAMTS) family (Kim et al., 2016). Most ADAMTSs are secreted proteases that cleave components in the extracellular matrix, and their malfunctions result in multiple diseases including cancer (Kelwick et al., 2015). Sona is positively involved in Wingless (Wg) signaling, and secreted by both the exosomal secretion pathway and Golgi transport (Kim et al., 2016; Won et al., 2019). Sona cleaves the linker region of extracellular Wg and generates a new functional form of Wg that is specialized in cell proliferation (Won et al., 2019).

Sona is important for cell survival, with the level of Sona correlated with the extent of cell survival (Tsogtbaatar et al., 2019). Cells expressing a high level of *sona* are cell autonomously resistant to γ-ray irradiation, while Sona secreted from these cells induces Cyclin D (Cyc D) in the neighboring cells for cell survival and proliferation in a non-cell autonomous manner. Interestingly, Wg-CTD but not full-length Wg induces Cyc D, which demonstrates that Sona is involved in intercellular communication to support the normal development of damaged tissues by regulating Wg signaling. Consistent with this, *sona* suppressors such as *wntless*, *arrow*, *pou domain motif 3*, and *archipelago* are related to Wg signaling (Han et al., 2020; Kim and Cho, 2020; Kim et al., 2016; Nam and Cho, 2020; Won et al., 2019).

We report here that Ana3 is also important for cell survival. Furthermore, overexpression of Ana3 increased the survival rate of irradiated flies, and the amount of Ana3 correlated with the extent of organism survival under irradiation. The level of Ana3 in wing discs was significantly increased by 1 h after irradiation, indicating that Ana3 may be one of the proteins that respond to irradiation at the front line. Ana3 expressed in S2 cells increased the level of both intracellular and secreted Sona by negatively regulating the lysosomal degradation pathway, which is consistent with the finding of *ana3*^{m19} as a *sona* suppressor. Our data demonstrate a new role of Ana3 in the stabilization of Sona.

MATERIALS AND METHODS

Fly lines

GMR-Grim, *UAS-p35*, and *Gal4* drivers including *ptc-Gal4*, *nub-Gal4*, *GMR-Gal4*, *en-Gal4*, and *act-Gal4* were obtained from Bloomington Drosophila Stock Center (USA). *UAS-ana3 RNAi* line was obtained from VDRC (V101280). *Ubq-ana3-GFP*, *UAS-ana3-GFP*, and *ana3*^{SH0558} flies were kindly provided by Jordan W. Raff. *UAS-sona* lines were generated in our laboratory (Kim et al., 2016). Flies were incubated at 25°C unless otherwise indicated.

Adult wing mounting and size measurement

Wings of adult flies less than 3 days old were dissected and mounted in Gary's Magic Mountant (Mixture of Canada Balsam and methyl salicylate, 4:1). For wing size, the entire wing except for the hinge region was measured as pixel numbers with ImageJ.

Cell culture, transfection, and preparation of various fractions

S2 cell lines obtained from DGRC were cultured in M3 media (S8398; Sigma-Aldrich, USA) containing 10% insect medium supplement (I7267; Sigma-Aldrich) at 25°C. Transfection was performed with cellfectin (Invitrogen, USA) according to the manufacturer's instruction. *pUAST-sona-HA* (Kim et al., 2016) and *pUAST-ana3-GFP* (Stevens et al., 2009) were used for transfection.

To prepare the P100 fraction, conditioned media (CM) were sequentially centrifuged at 300*g*, 2,000*g*, 10,000*g* to remove dead cells and cell debris (Gross et al., 2012). The cleared CM was centrifuged at 100,000*g* to obtain two fractions. The supernatant fraction (SN_Δ) containing soluble proteins was concentrated with an Amicon ultra-4 centrifugal filter unit (Millipore, USA) for further analysis. The pellet P100 fraction containing extracellular vesicles including exosomes was washed with phosphate-buffered saline (PBS) and then pelleted again by one additional centrifugation at 100,000*g* to remove contaminants.

Immunocytochemistry

Sona-Pro and Sona-C antibodies were used to detect Sona protein as previously described (Kim et al., 2016). The Ana3 antibody was generously provided by Jordan W. Raff. For intracellular staining, fly larvae were dissected and fixed with PLP solution (2% paraformaldehyde, 0.1 M lysine, 0.25% sodium M-periodate) as described (McLean and Nakane, 1974). Fixed wing discs were blocked in block buffer (50 mM Tris pH 6.8, 150 mM NaCl, 0.5% NP-40, 5 mg/ml bovine serum albumin [BSA]) for 2 to 6 h at 4°C and washed in wash buffer (50 mM Tris pH 6.8, 150 mM NaCl, 0.5% NP-40, 1 mg/ml BSA). Antibodies were diluted in wash buffer and incubated overnight at 4°C or 2 h at room temperature. After washing several times, samples were treated with DAPI and mounted with a Vectashield mounting medium. Sample images were captured with an LSM laser (Zeiss, Germany) scanning confocal microscope and processed by Adobe Photoshop. Sona-Pro (rabbit, 1:200), Sona-C (mouse, 1:100), Ana3 (Stevens et al., 2009) (rabbit, 1:100), and cleaved Dcp-1 (Cell signaling Asp216, rabbit, 1:100) were used.

For extracellular staining, larvae were dissected in ice cold M3 medium and incubated in M3 medium containing primary antibody for 2 h at 4°C as described in (Strigini and Cohen,

2000). Then, wing discs were washed with M3 media and PBS twice each and fixed in 4% paraformaldehyde in PBS for 50 min. Samples were then processed the same way as described above, except that the buffers did not contain any detergent. The antibodies were used at a 10-time higher concentration for extracellular staining than for intracellular staining.

Western analysis

Western analysis was performed as described (Kim et al., 2016). Protein bands were visualized with West Pico Plus Chemiluminescent Substrate (Thermo Scientific, USA) for an ECL system (Kim et al., 2016). Sona-Pro (rabbit, 1:5,000), HA (Roche 3F10, rat, 1:2,000), Ana3 (Stevens et al., 2009) (rabbit, 1:1,000), Syntaxin 1A (DSHB 8C3, mouse, 1:1,000), GAPDH (MA5-15738, mouse, 1:2,000; Invitrogen), and α-tubulin (T9026, mouse, 1:5,000; Sigma-Aldrich) were used. All samples except Ana3 were loaded in 10% SDS-PAGE gel. Samples for the Ana3 blot were loaded in 7% SDS-PAGE gel.

Irradiation condition

Flies were cultured at 25°C and irradiated during the second or third instar larval stage at the indicated γ-ray doses with a Gammacell 3000. They were cultured and dissected at the designated time or at the late 3rd instar larval stage for immunocytochemical analysis.

Statistical analysis

Statistical analysis was performed based on Student's *t*-test to compare controls with experimental groups by using oneway analysis of variance (ANOVA). Data are pre-sented as mean ± SD. The *t*-tests were used to determine the statistical significance of the difference between two groups. A P value < 0.05 was considered statistically significant.

RESULTS

The *m19 sona* suppressor has a lethal mutation in the *ana3* gene

We previously reported an ethyl methanesulfonate (EMS)-based genetic screen for the identification of suppressors in their heterozygous forms that survive against lethality induced by an overexpression of Sona (Kim and Cho, 2020; Kim et al., 2016). One of the suppressors, *m19*, was chosen among the 28 established *sona* suppressors for this study in order to understand the role of the *m19* gene in Sona function.

The *m19* was embryonic lethal, and its lethal site was mapped between *cinnabar* (*cn*) and *curved* (*c*) on the right

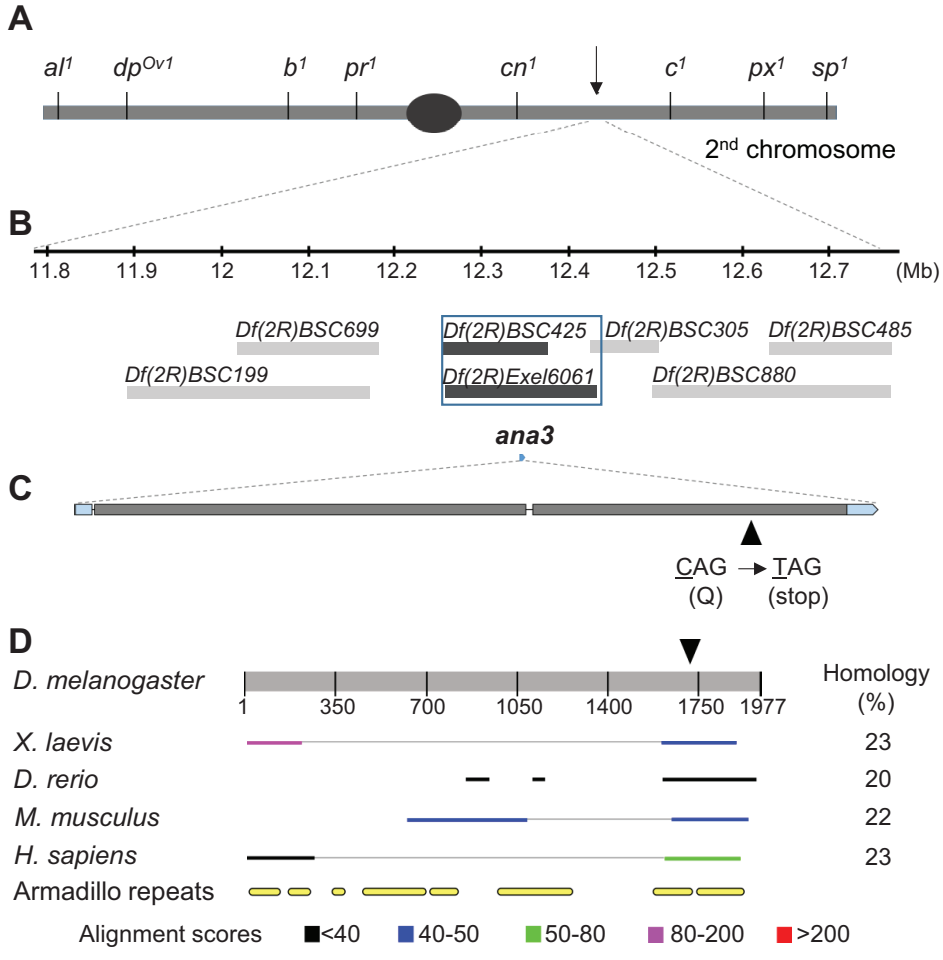

Fig. 1. Mapping of *ana3*^{m19} and comparison between Ana3 homologs. (A-C) Localization of the *m19* suppressor between *cn* and *c* by meiotic mapping (arrow in A). Deficiency mapping localized *m19* in the region between 48F1 and 49A1 (blue box in B). Whole-genome sequencing identified a C to T transition in the 5175th bp of the *ana3* gene of the *m19* suppressor (arrowhead in C). (D) Comparison between Ana3 homologs. Armadillo repeats are shown. The sequence homology in the truncated region of Ana3^{m19} protein is listed on the right, as indicated by alignment scores. *D. melanogaster*, *Drosophila melanogaster*; *X. laevis*, *Xenopus laevis*; *D. rerio*, *Danio rerio*; *M. musculus*, *Mus musculus*; *H. sapiens*, *Homo sapiens*.

arm of the second chromosome by meiotic mapping (Fig. 1A). Deficiency mapping located the lethal site of *m19* in the region between 48F1 and 49A1 that is deleted in *Df(2R)BSC425* and *Df(2R)Exel6061* (Fig. 1B). In this region, 11 genes were present, so we carried out complementation tests by crossing *m19* and available mutants in these genes. We identified $ana3^{SH0558}$, a loss of function mutant of *ana3* that does not complement the lethality of *m19* (Stevens et al., 2009). Although the homozygous $ana3^{SH0558}$ was pupal lethal, the transheterozygous *m19*/$ana3^{SH0558}$ was embryonic lethal because *m19* is more severe than $ana3^{SH0558}$ in the loss of the *ana3* phenotype.

Whole-genome sequencing revealed that *m19* has a single base change from C to T near the end of the *ana3* coding region (Fig. 1C). This mutation changed a glutamine residue to a stop codon that truncates 252 amino acid residues at the carboxyl terminal region from the total 1,977 amino acid residues of wild-type Ana3 (Fig. 1D). This truncated region was the most conserved region in Ana3 homologs in other model organisms, showing 20% to 23% identity and 34% homology and containing Armadillo repeats (Song et al., 2003). Ana3 had at least eight different regions containing multiple Armadillo repeats (Fig. 1D).

Knockdown of *ana3* results in small and deformed wings and hinges

To test whether the *m19* suppressor is indeed *ana3*, we examined the loss and gain of Ana3 effects on Sona. Before we initiated this work, we confirmed that *Ubq-ana3-GFP*, *UAS-ana3-GFP*, and *UAS-ana3 RNAi* lines were effective in changing the level of Ana3 protein (Supplementary Fig. S1). Overexpression of Ana3 in *actin-Gal4>UAS-ana3-GFP* (*act>ana3-GFP*) and *Ubq-ana3-GFP* flies induced no morphological changes (Figs. 2A-2C). In contrast, knockdown of *ana3* in *tubulin>ana3 RNAi* (*tub>ana3i*) flies induced embryonic lethality. Therefore, the gain of Ana3 did not affect fly morphology, but the loss of Ana3 caused developmental defects.

Knockdown of Ana3 induced morphological changes in wings and hinges. Wings of *cubitus interruptus (ci)>ana3i*, *patched (ptc)>ana3i*, and *engrailed (en)>ana3i* flies at 25°C were smaller than control wings by 29%, 35%, and 14%, respectively, and those of *nub>ana3i* flies remained folded (Figs. 2D-2J, Supplementary Figs. S2A and S2B). The size of the wings was decreased throughout the entire blade regardless of the *Gal4*-expressing regions but more so along the proximodistal axis than the anteroposterior axis (Figs. 2D-2I). Knockdown of *ana3* with *nub-Gal4* and *ptc-Gal4* at 29°C induced more severe phenotypes than at 25°C (Supplementary Fig. S2). In addition, female *ptc>ana3i* flies were pupal lethal at 29°C with only 3% escapers while male *ptc>ana3i* flies with small wings were not lethal, showing that knockdown of *ana3* induced more severe phenotypes in females than in males (Fig. 2J, Supplementary Figs. S2C-S2F).

Ana3 was also important for the growth in the region between the hinge and the anterior cross vein. Compared to control hinges, hinges of *ci>ana3i*, *ptc>ana3i*, and *en>ana3i* flies were significantly smaller due to the reduction in the size of the anterior costal cells, alula, and 1st basal cells (Fig. 2K). In sum, Ana3 is important for the development and growth of wings and hinges (Figs. 2K-2N).

ana3 and *sona* show a mutually positive genetic interaction

To examine the genetic interaction between *sona* and *ana3*, we then examined whether the knockdown of *ana3* also rescues the lethality induced by *sona* overexpression, because $ana3^{m19}$ as a heterozygous form successfully rescued the lethal phenotype of *sona* overexpression in the original genetic screen (Fig. 3A). All *ptc>sona* flies were embryonic lethal and 79% of *ptc>ana3i* flies developed to adults at 25°C. In contrast, 85% of *ptc>sona; ana3i* flies survived to adults. Similarly, all *en>sona* flies were embryonic lethal and 88% of *en>ana3i* flies developed into adults, while 90% of *en>sona; ana3i* flies developed into adults (Fig. 3A). Thus, knockdown of *ana3* substantially rescued the Sona-induced lethal phenotype.

Coexpression of *sona* reciprocally rescued the small wing phenotype caused by knockdown of *ana3*. The small wing phenotype of *ptc>ana3i* and *en>ana3i* flies was rescued up to 99% and 94% by the coexpression of *sona*, respectively (Figs. 3B-3H). The small hinge phenotype of *en>ana3i* flies was also partially rescued in 20% of *en>ana3i; sona* adult flies (n = 20, Fig. 3G). Based on this mutually positive genetic interaction between *ana3* and *sona*, as well as the failed complementation between *m19* and $ana3^{SH0558}$, we concluded that the suppression of the Sona-induced lethality in *m19* is due to a lethal mutation in the *ana3* gene, which we name $ana3^{m19}$.

Loss of *ana3* results in apoptosis

Sona as well as some centrosomal proteins such as CEP-55 and RassF7 is important for cell survival (Gulsen et al., 2016; Kalimutho et al., 2018; Tsogtbaatar et al., 2019). Based on the close genetic relationship between *ana3* and *sona*, we tested whether the small wing phenotype by knockdown of *ana3* is also due to cell death. Indeed, dying cells with activated Death caspase 1 (Dcp-1) were detected in *en>ana3i* wing discs (Figs. 4A and 4B). When *ana3i* and *p35* were coexpressed by *en-Gal4*, the Dcp-1 signal disappeared, establishing that knockdown of *ana3* induces apoptosis (Figs. 4C and 4D).

To examine whether the inhibition of cell death by the caspase inhibitor p35 rescues the adult wing phenotype induced by the knockdown of *ana3*, we compared wings of *en>ana3i; p35* flies to those of *en>ana3i* and *en>p35* flies at 29°C (Figs. 4E-4H). In fact, the wing size of *en>GFP, ana3i; p35* flies was 93% of the control wings, whereas those of *en>GFP, ana3i* and *en>GFP, p35* were only 77% and 67% of the control wings, respectively (Fig. 4I). Knockdown of *ana3* rescued defects in both the shape and the size of the wings and hinges caused by *p35* overexpression (Figs. 4E-4H). Thus, apoptosis is responsible for the phenotypes induced by the knockdown of *ana3*.

We then asked whether overexpression of *ana3* can suppress the cell death induced by the overexpression of Grim, one of apoptotic proteins (Chen et al., 1996). *GMR>Grim/+* flies had small and rough eyes, but *GMR>Grim; ana3-GFP* flies had normal eyes just slightly smaller than control *GMR/+*

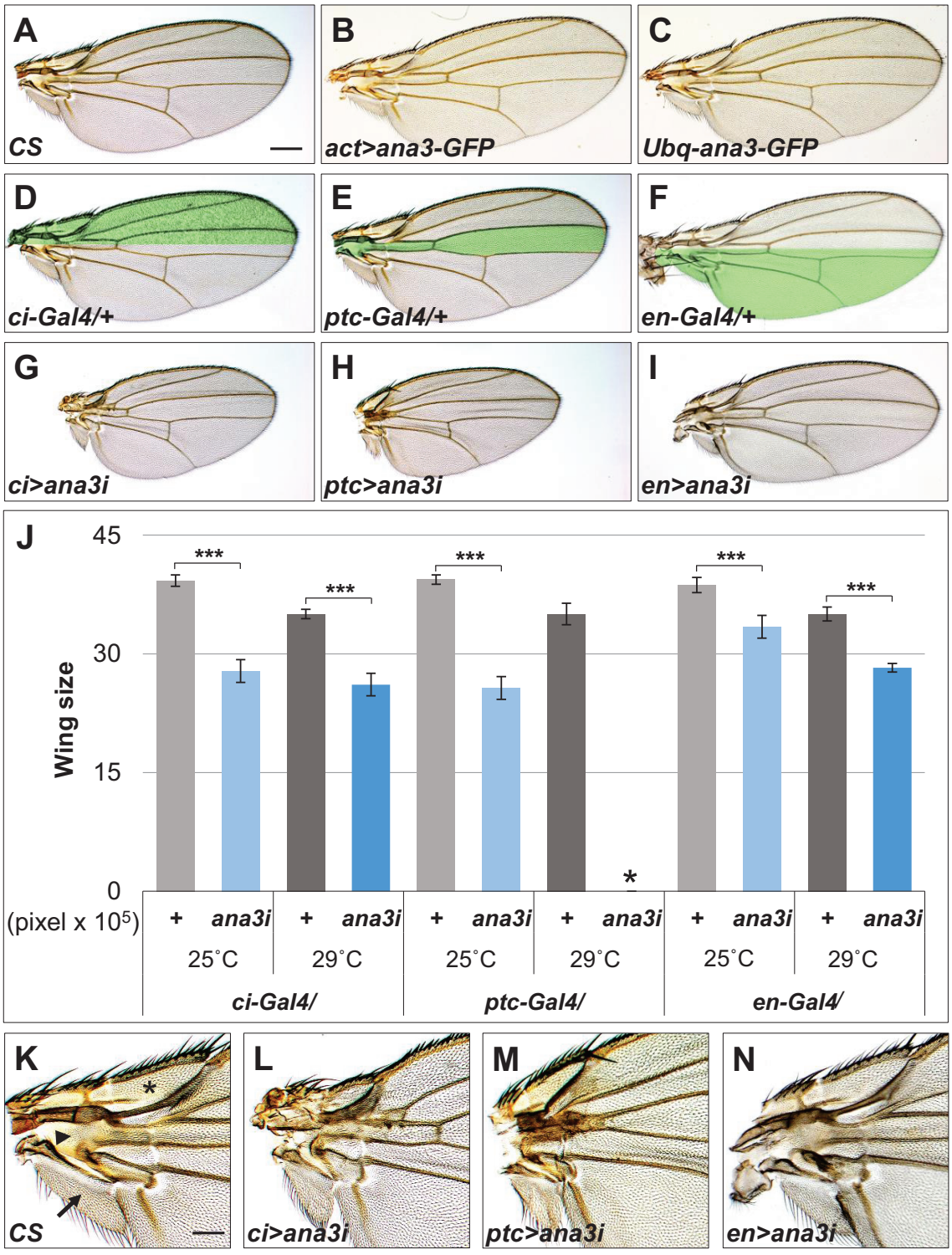

Fig. 2. Loss of *ana3* causes developmental defects in wings and hinges. All wings are obtained from female flies cultured at 25°C. Their genotypes are given in the lower left in all panels. (A-C) Gain of *ana3* phenotype in *act>ana3-GFP* and *Ubq-ana3-GFP* wings compared to *CS*. (D-I) Knockdown of ana3 phenotype. *CS* and *UAS-ana3i* lines were crossed with *ci-Gal4*, *ptc-Gal4*, and *en-Gal4* drivers, and the adult wings of the progenies were compared. The expression regions of *Gal4* drivers are indicated in green (D-F). (J) Wing sizes of the flies in (D-I) were measured as pixel numbers ($n > 30$ for each) using the entire wing blade except for the hinge with ImageJ. 100% lethality is marked with the single asterisk. (K-N) Developmental defects in the hinges of *ana3* knockdown flies. In (K), the three major parts of the hinge are marked as follows: anterior costal cell with an asterisk, 1st basal cells with an arrowhead, and the alula with an arrow. Scale bars = 200 μm (A-I); 71 μm (K-N). ***$P < 0.001$.

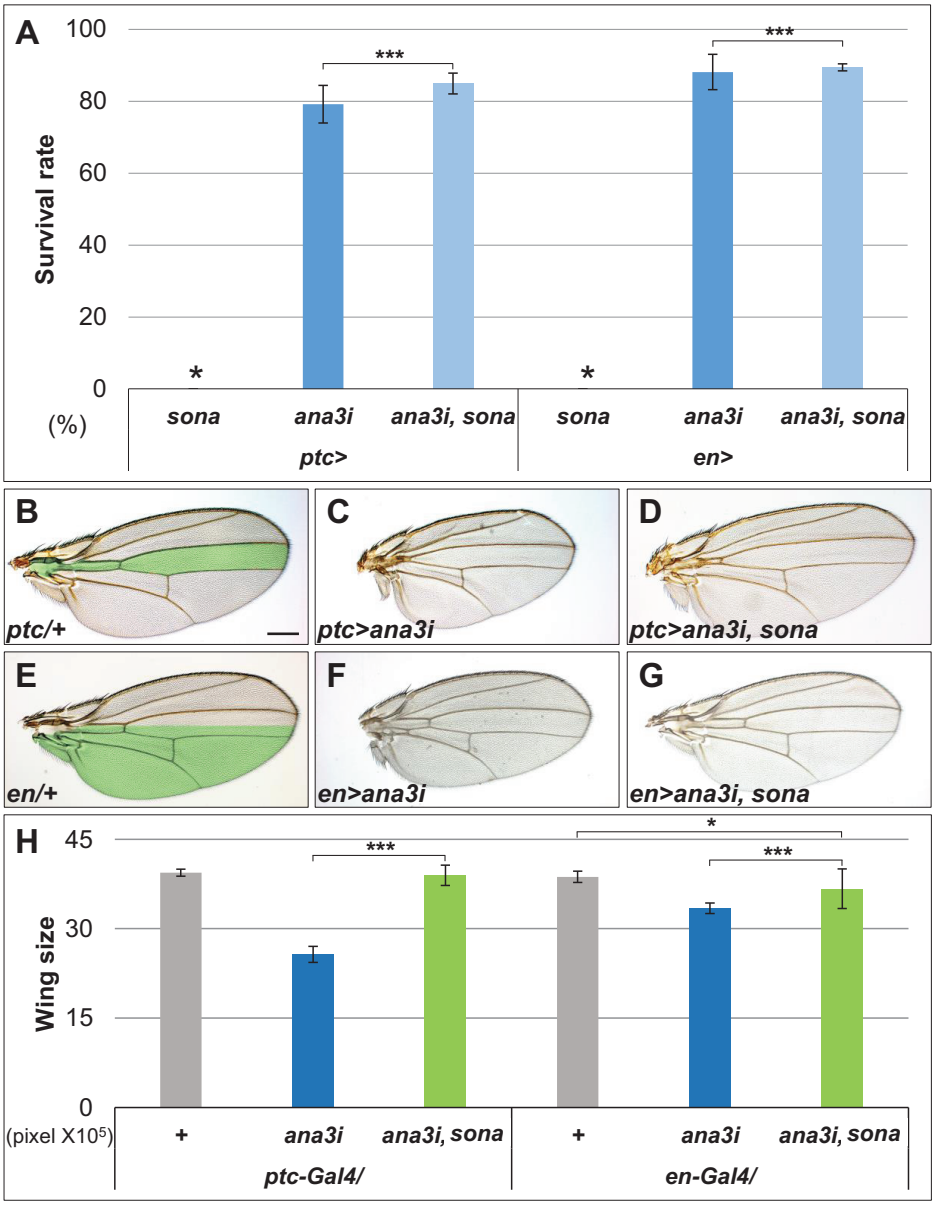

Fig. 3. *sona* and *ana3* have a positive genetic interaction. (A) Lethality by overexpressed Sona is rescued by coexpression of *ana3i*. The single asterisk indicates 100% pupal lethality of *ptc>sona* and *en>sona* flies. Survival rates from two independent experiments are averaged (n > 100, each). Lethality by *UAS-sona* expression is similar to that by *UAS-sona; UAS-GFP*, establishing that lethality caused by Sona overexpression is not affected by UAS gene dose (Han et al., 2020). (B-H) The small wing phenotype by knockdown of *ana3* is rescued by overexpression of Sona. Wings from flies with marked genotypes are shown in (B-G). The expression regions of *Gal4* drivers are indicated in green in (B and E). Wing sizes were measured and averaged in the same way as in Fig. 2J (n > 20 for each) (H). Scale bar = 200 μm (B-G). $*P < 0.1$ (H), $***P < 0.001$ (A and H).

eyes (Supplementary Figs. S3A-S3C). This result raised an interesting possibility that Ana3 may actually promote cell survival in cell-death-causing conditions.

Overexpression of Ana3 increases cell survival

We previously reported that the gain of Sona is capable of promoting organism survival under irradiation (Tsogtbaatar et al., 2019). To test whether the gain of Ana3 is also able to promote organism survival, we irradiated *Ubq-ana3-GFP*, *CS*, and $ana3^{SH0558}$/*CyO-GFP* larvae at 1,000, 1,250, and 1,500 rad, and counted the number of adult survivors to obtain survival rates (Fig. 5A). The survival rate of $ana3^{SH0558}$/*CyO-GFP* flies was only 47%, while those of *Ubq-ana3-GFP* and *CS* flies were about 90% in the unirradiated condition (Fig. 5A, the darker set of bars). To compare the survival rates of these flies in unirradiated vs. irradiated conditions, the survival rates in the unirradiated condition were converted to 100%. At 1,000 rad, the survival rates of both *Ubq-ana3-GFP* and *CS* flies were 97% but that of $ana3^{SH0558}$ heterozygotes was only 51%, showing that the half amount of Ana3 in $ana3^{SH0558}$ heterozygotes is insufficient to resist radiation damage. At 1,250 rad, the survival rate of *Ubq-ana3-GFP* was 80%, while those of *CS* and $ana3^{SH0558}$ heterozygotes were 46% and 36%, respectively, showing that the high level of Ana3 in *Ubq-ana3-GFP* flies is responsible for survival against radiation damage. At 1,500 rad, over 90% of all flies died regardless of genotype.

Consistent with the role of Ana3 in survival against radiation, *CS* wing discs had a high level of Dcp-1 signals while *Ubq-ana3-GFP* wing discs had no Dcp-1 signals 24 h after irradiation at 1,500 rad (Figs. 5B and 5C). Furthermore, *Ubq-ana3-GFP* flies developed one day earlier than *CS* flies in both

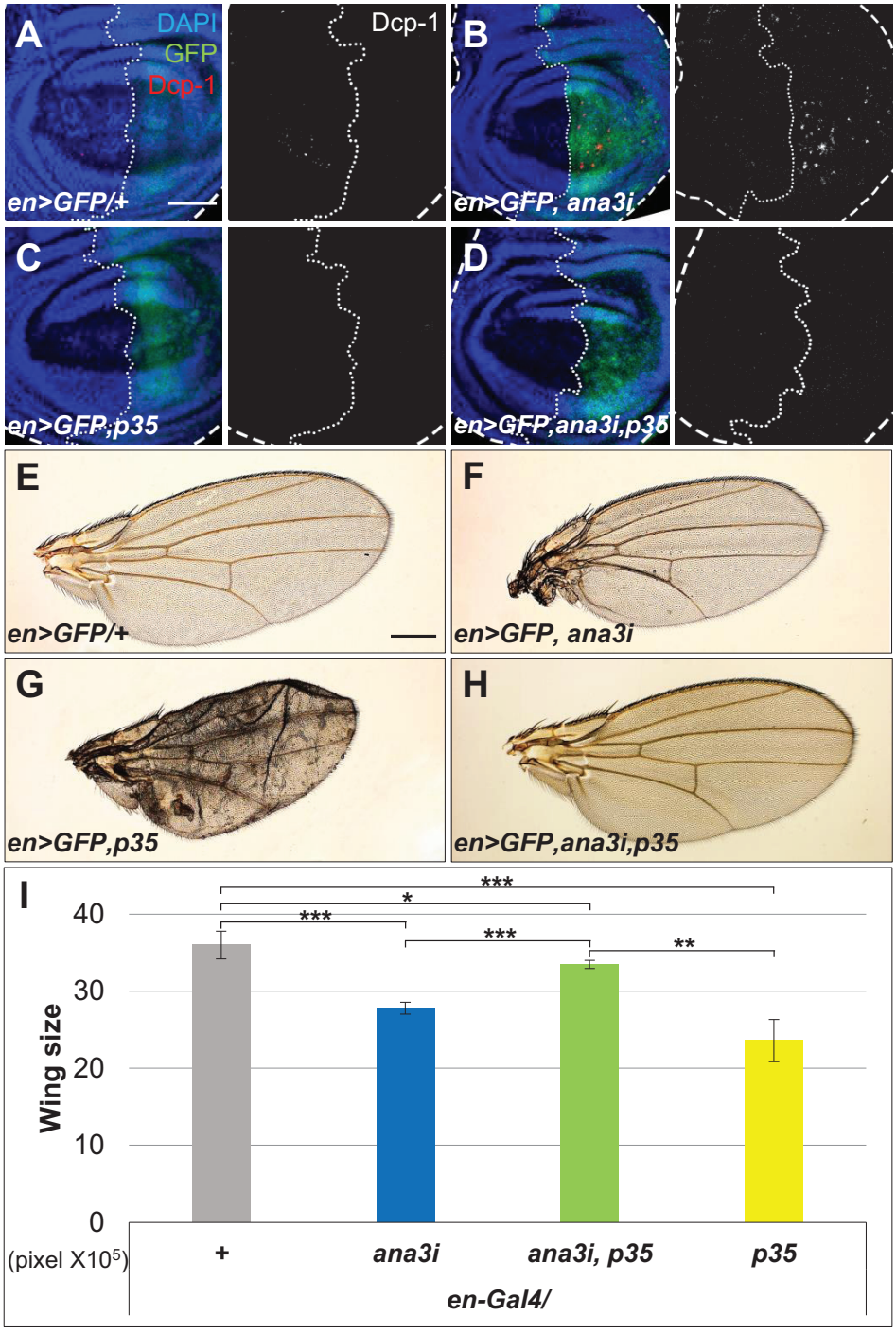

Fig. 4. Loss of *ana3* induces apoptosis. (A-D) Knockdown of *ana3* induces cell death but the coexpression of p35 rescues the cell death phenotype. *CS*, *UAS-ana3i*, *UAS-p35*, and *UAS-ana3i; UAS-p35* lines were crossed with the *en-Gal4 UAS-GFP* driver and incubated at 29°C. Apoptotic cells in the wing discs of larval progenies are visualized with Dcp-1. The *Gal4* expressing region is marked with GFP. (E-I) The small wing phenotype by knockdown of *ana3* (F) is rescued by coexpression of p35 (H). Adult wings of the controls are shown in (E) and (G). Flies were crossed and incubated at 29°C. Wing sizes were measured and averaged in the same way as in Fig. 2J (n > 10 for each) (I). The *en>GFP, p35* wings were small and defective, similar to previous reports that overexpression of p35 causes developmental defects in eyes and wings (Katanayeva et al., 2010; Nguyen et al., 2016). Scale bars = 50 μm (A-D); 239 μm (E-H). $*P < 0.1$, $**P < 0.01$, $***P < 0.001$.

unirradiated and irradiated conditions (Supplementary Fig. S3D). In case of 4,000 rad, *Ubq-ana3-GFP* flies entered the pupal stage two days earlier than the *CS* flies. In sum, Ana3 can increase survival rates under irradiated conditions and accelerate fly development.

To confirm whether the amount of Ana3 correlates with the survival rate, we carried out the following experiment including *act>ana3-GFP* larvae that express a larger amount of Ana3 than *Ubq-ana3-GFP* (Supplementary Figs. S4A-S4D). *CS*, *Ubq-ana3-GFP*, and *act>ana3-GFP* larvae were irradiated with γ-rays and their survival rates were measured (Supplementary Fig. S4E). At 1,500 rad, the survival rates of *CS* and *Ubq-ana3-GFP* were below 10% but that of *act>ana3-GFP* was 67%. At 2,000 rad, the survival rates of *CS* and *Ubq-ana3-GFP* flies were less than 5% but that of *act>ana3-GFP* flies was 16%. These results demonstrate that the amount of Ana3 correlates with the survival rate of irradiated flies.

If the amount of Ana3 correlates with the survival rate against irradiation, it is possible that irradiation triggers an increase in the amount of Ana3. Indeed, the level of Ana3 in

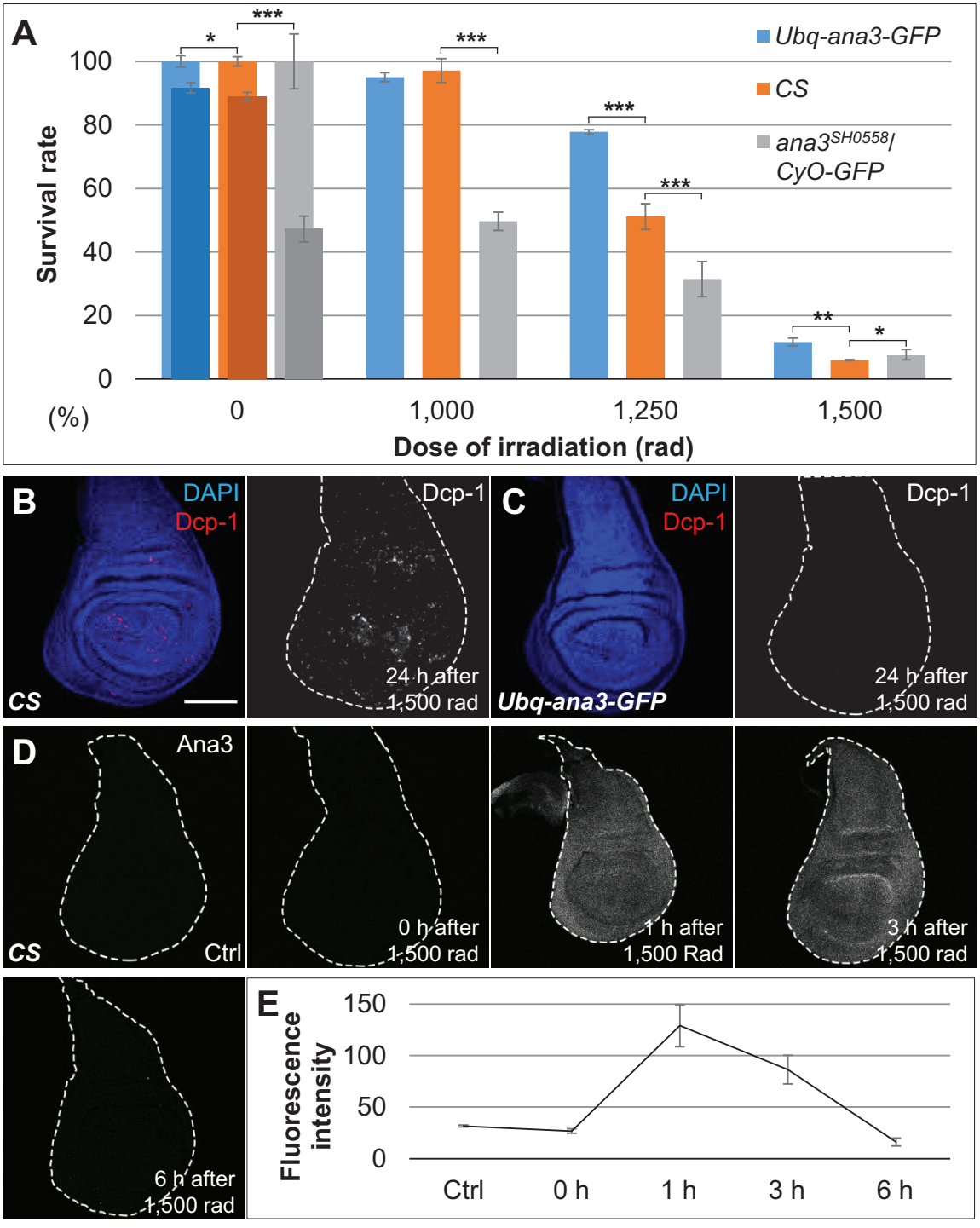

Fig. 5. Ana3 promotes cell survival. (A) Number of adult survivors correlates with the amount of Ana3. *Ubq-ana3-GFP*, *CS*, and *ana3*^{SH0558}*/CyO-GFP* larvae were irradiated with 1,000, 1,250, and 1,500 rad during 2nd to 3rd instar larval stages, and the number of adults was divided by the number of total empty pupal cases to obtain survival rates. The actual survival rates of unirradiated *Ubq-ana3-GFP*, *CS*, and *ana3*^{SH0558}*/CyO-GFP* are indicated with the darker set of bars. To compare the survival rates of these flies after irradiation, the survival rate of the irradiated flies was divided by that of the unirradiated flies to obtain a normalized survival rate. Three independent experiments were carried out with more than 100 flies for each genotype and irradiation intensity. (B and C) Ana3 reduces the amount of activated Dcp1. *CS* and *Ubq-ana3-GFP* 3rd instar larvae were dissected 24 h after irradiation. (D and E) Irradiation increases the level of Ana3 in the wing discs of irradiated flies. *CS* 3rd instar larvae were dissected before and right after irradiation, as well as 1 h, 3 h, and 6 h after irradiation, and their wing discs were immunostained to visualize Ana3 (D). The fluorescence intensity of each imaginal disc was measured with ImageJ and averaged ($n \geq 15$ for each) (E). Ctrl, control. Scale bar = 100 μm (B-D). $*P < 0.1$, $**P < 0.01$, $***P < 0.001$.

CS wing discs was increased 4 times in 1 h and then reduced to the normal level 6 h after irradiation (Figs. 5D and 5E). This shows that the amount of Ana3 is dynamically regulated by irradiation, which may be prerequisite for cell survival against irradiation.

Both intra- and extracellular levels of Sona are decreased in *ana3* mutants

Since overexpression of Sona also increases the survival rate of flies after irradiation (Tsogtbaatar et al., 2019), and *ana3* has a positive genetic interaction with *sona*, we reasoned that the level of Ana3 may correlate with that of Sona *in vivo*. We therefore examined the amount of Sona in *CS* and *ana3*^{SH0558} wing discs visualized with two anti-Sona antibodies, Sona-Pro antibody that recognizes the pro domain and Sona-C antibody that recognizes the carboxyl region (Kim et al., 2016). Intracellular levels of Sona in *ana3*^{SH0558} wing discs were lower than those in control discs by 29% and 40% with Sona-Pro and Sona-C antibodies, respectively, whereas the levels of Dlg were similar (Figs. 6A-6I, Supplementary Fig. S5). Furthermore, the extracellular levels of Sona in *ana3*^{SH0558} wing discs visualized by Sona-Pro were only one fourth of control wing

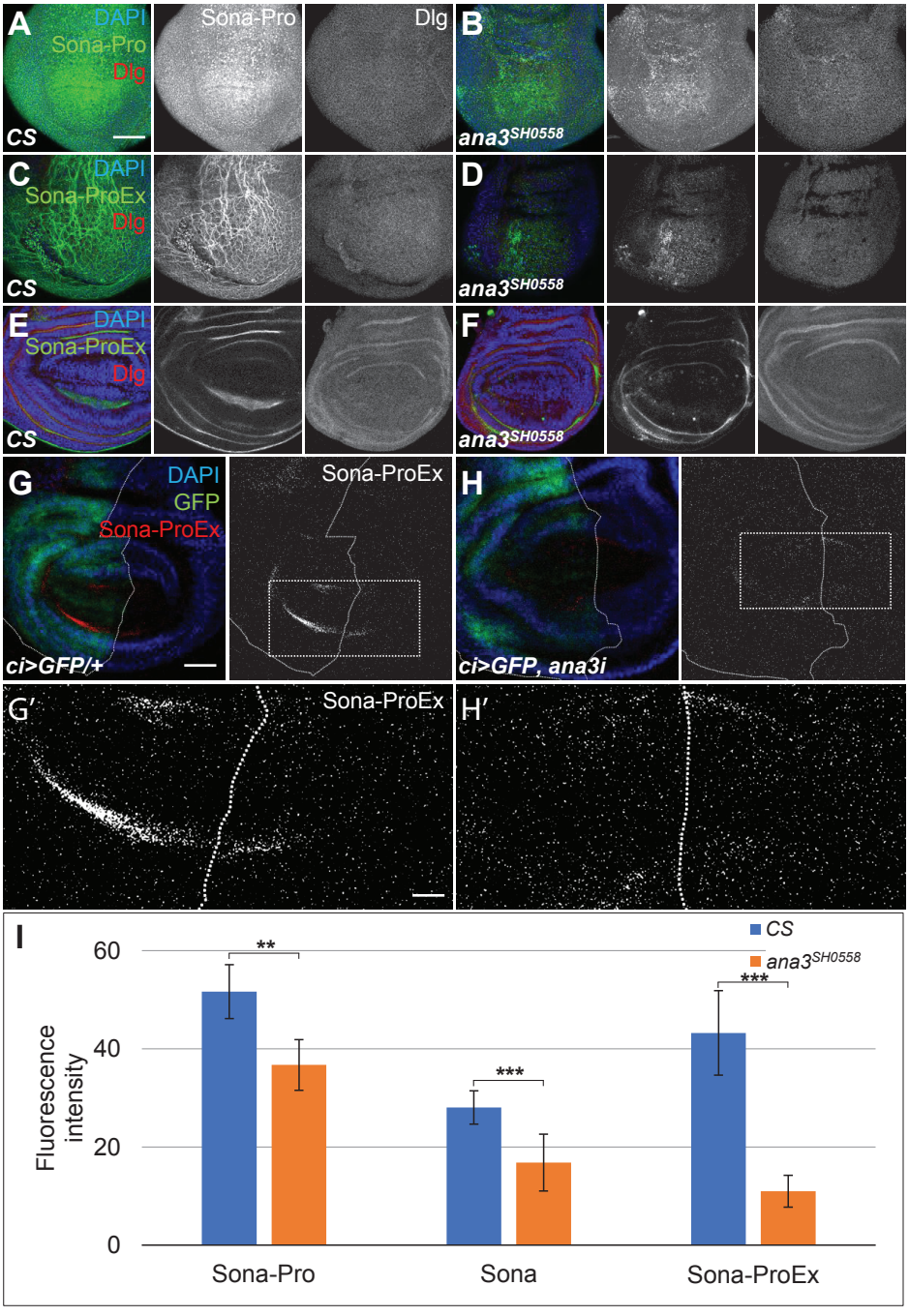

Fig. 6. Knockdown of *ana3* decreases the level of Sona in both intra- and extracellular regions of wing discs. (A-F) Loss of *ana3* decreases the level of Sona in both intracellular and extracellular regions. Sona is visualized in the wing discs of *CS* and *ana3*^{SH0558} 3rd instar larvae with Sona-Pro antibody. Dlg is visualized with Dlg antibody (Cho et al., 2000) to show no change in the protein level unlike Ana3. Intracellular Sona in the apical disc proper (A and B) and extracellular Sona in the peripodial epithelium (C and D) and the basal region (E and F) of *CS* and *ana3*^{SH0558} wing discs were compared. (G and H) *CS* and *ana3i* flies were crossed with *ci-Gal4* flies and dissected at late 3rd instar larval stage for extracellular immune-staining of Sona with Sona-Pro antibody. For more precise comparison, regions inside the white boxes in (G and H) were magnified (G' and H'). Sona visualized by Sona-C antibody is presented in Supplementary Fig. S6, and the intensities of these wing discs were measured by ImageJ and plotted in (I). Scale bars = 50 μm (A-F); 33 μm (G and H); 11 μm (G' and H'). $^{**}P < 0.01$, $^{***}P < 0.001$.

discs in the peripodial epithelium (Figs. 6C and 6D). The level of extracellular Sona in the basal region of the disc proper was also substantially reduced in *ana3*^{SH0558} wing discs (Figs. 6E and 6F). When the level of Ana3 is reduced in the anterior region of *ci<GFP*, *ana3i* discs, the extracellular level of Sona was also reduced (Figs. 6G, 6G', 6H, and 6H'). Therefore, the level of Ana3 positively correlates with that of both intra- and extracellular Sona, suggesting that Ana3 regulates the level of Sona *in vivo*.

Ana3 is secreted via exosomes

To biochemically verify the role of Ana3 in regulating the *in vivo* level of Sona, we utilized the S2 cell culture system. S2 cells transfected with *actin-Gal4* and different combinations of *UAS-ana3-GFP* and *UAS-sona-HA* plasmids were cultured for 3 days, and then the CM after removal of dead cells and cell debris was centrifuged at 100,000*g* for 3 h to obtain two fractions: the P100 pellet fraction that contains exosomes and the supernatant SN_{Δ} fraction that contains soluble extracellular proteins secreted by Golgi transport (Gross et al., 2012). The 225 kDa Ana3 protein endogenously expressed in S2 cells and the 252 kDa Ana3-GFP protein were detected in cell extract (CX) regardless of Sona (Fig. 7A). Both Ana3 forms were unexpectedly detected in the P100 fraction, indi-

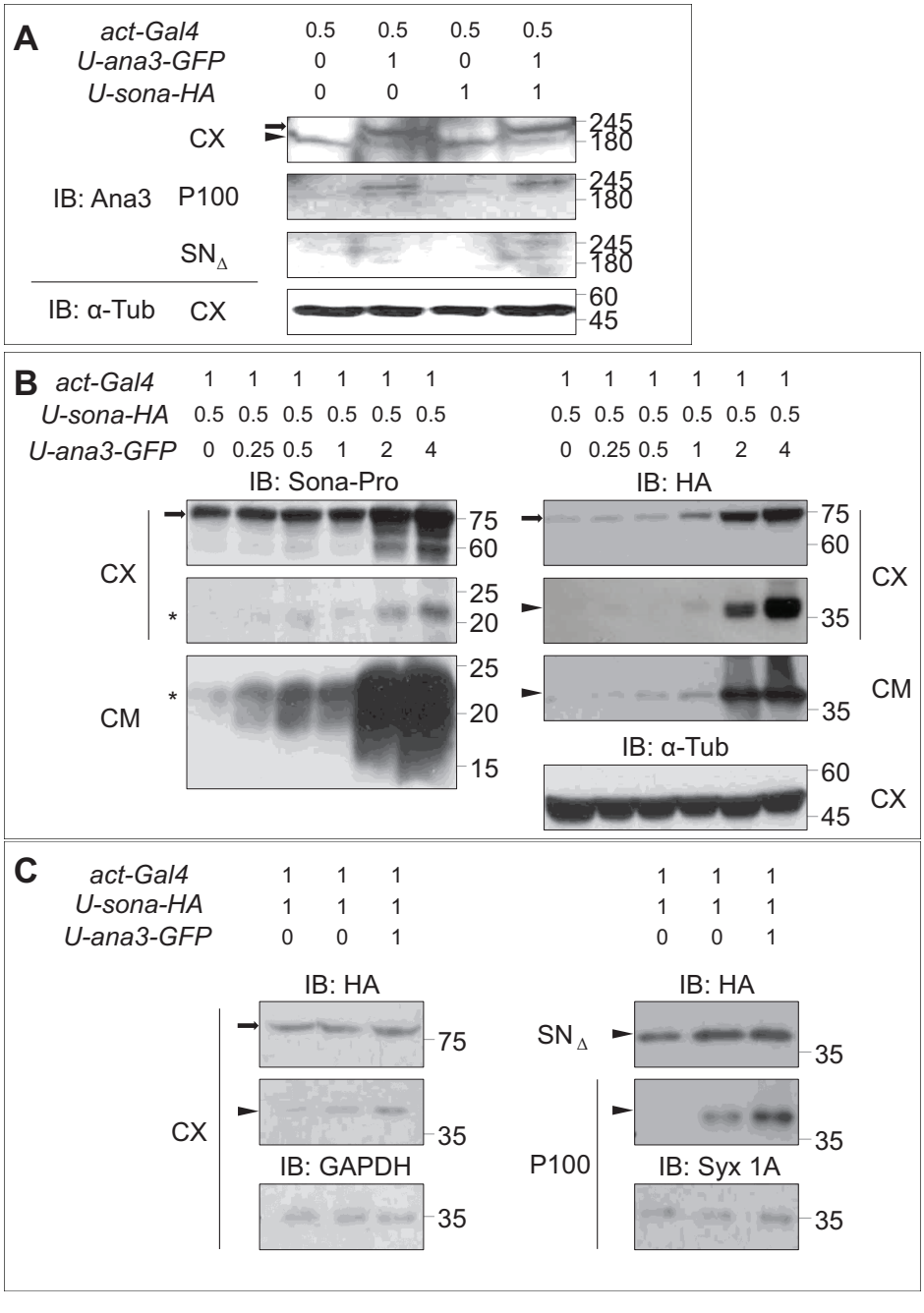

Fig. 7. Ana3 is secreted via exosomes and increases the level of exosomal Sona. In all western analyses, the fractions of cells are marked on the left, and the names and amounts (μg) of DNA constructs transfected to the S2 cells are given on the top of each panel. Antibodies used for immunoblots (IB) are indicated. (A) Ana3 is secreted via exosomes. The 252 kDa band indicates Ana3-GFP (arrow) and the 225 kDa band indicates endogenous Ana3 (arrowhead). Ana3 is detected in both P100 exosomal fraction and SN_{Δ} fraction. (B) Ana3 stabilizes Sona. S2 cells were co-transfected with increasing amounts of *ana3-GFP* and a constant amount of *sona-HA* cDNA, and the levels of Sona in CX and cleared conditioned media (CM) were compared. The 75 kDa full-length Sona (arrows) was detected with Sona-Pro antibody or anti-HA antibody. The 37 kDa active Sona (arrowheads) was detected with anti-HA antibody. The 22 kDa cleaved pro-domain of Sona (asterisks) was detected by Sona-Pro antibody. (C) Ana3 significantly increased the level of Sona in P100 but not in SN_{Δ} or CX fraction. The 75 kDa full-length Sona (arrow) and the 37 kDa active Sona (arrowheads) were detected with anti-HA antibody. The 37 kDa GAPDH and the 35 kDa Syntaxin 1A (Syx1A) were used as a cytoplasmic marker and an exosomal marker, respectively.

cating that Ana3 is secreted to extracellular space. Endogenous Ana3 secreted from untransfected S2 cells demonstrated that the presence of Ana3 in the P100 fraction is not due to the overexpression of Ana3 (second row in Fig. 7A). Most extracellular Ana3 was present in the P100 fraction, although some faint bands were detected in the SN_{Δ} fraction. Therefore, we concluded that extracellular Ana3 is secreted mostly via exosomes.

Ana3 increases the level of exosomal Sona by protein stabilization

To find out whether Ana3 regulates the level of Sona in S2 cells, S2 cells were transfected with increasing amounts of *UAS-ana3* cDNA with a constant amount of *UAS-sona-HA* and *act-Gal4* cDNAs. We previously reported that 75 kDa full-length Sona is processed intracellularly, while 37 kDa active Sona and 20 to 25 kDa pro domain fragments are secreted to the extracellular space by both the exosomal secretion pathway and conventional Golgi transport (Won et al., 2019) (Fig. 7B). The 75 kDa full-length Sona-HA is detected by both Sona-Pro and anti-HA antibodies while 20 to 25 kDa pro domain fragments and 37 kDa active Sona-HA are detected by Sona-Pro and anti-HA antibody, respectively (Won et al., 2019) (Fig. 7B). The amounts of these Sona products in both CX and precleared CM were increased as the amount of Ana3 was increased. Since the transcription of transfected *sona* cDNA is carried out by Gal4 protein expressed by the actin promoter, the increase in the Sona level is due to the stabilization of Sona by Ana3 in S2 cells. Especially, the amounts of 20 to 25 kDa fragment and active Sona-HA were dramatically increased. This indicates that Ana3 specifically stabilizes active Sona in P100, SN_{Δ}, or both fractions.

We have previously shown that Arrow (Arr) secreted via exosomes can stabilize Sona when it is added to the culture media of Sona-expressing S2 cells (Han et al., 2020). Since both Ana3 and Arr stabilize exosomal Sona and are secreted via exosomes, we reasoned that exosomal Ana3 may also stabilize Sona. To test this possibility, we purified exosomes from the culture media of S2 cells transfected with *ana3* cDNA and then added the obtained exosome fraction to the culture media of S2 cells transfected with *sona* cDNA. Unlike exosomal Arr, however, exosomal Ana3 did not noticeably increase Sona stability (Supplementary Fig. S6).

To identify which fraction of extracellular Sona among P100 and SN_{Δ} fractions is increased by Ana3, the CM was further fractionated to P100 and SN_{Δ} fractions. Similar to the data in Fig. 7B, the level of full-length Sona was not noticeably changed when 0.5 to 1 μg of *UAS-ana3-GFP* and 1 μg of *UAS-sona-HA* (0.5 to 1:1 ratio) were co-transfected (arrow in the left panel of Fig. 7C), while the amount of active Sona slightly increased in CX (arrowhead in the left panel of Fig. 7C). Interestingly, the amount of active Sona-HA in the P100 fraction was greatly increased while that in the SN_{Δ} fraction showed little change (right panel of Fig. 7C). Therefore, Ana3 specifically increased the level of exosomal Sona when Sona is coexpressed with Ana3.

DISCUSSION

We have shown in this report that the *ana3*^{m19} mutant is a suppressor of Sona-induced lethality (Fig. 1). Fly *ana3* has a positive genetic interaction with *sona* that encodes a metalloprotease involved in Wnt signaling, establishing a potential link between Ana3/RTTN and Wnt signaling. Ana3/RTTN is a peripheral member of the centrosome complex whose malfunction leads to embryonic lethality in both *ana3* mutant flies and *RTTN* knockout mice (Faisst et al., 2002; Stevens et al., 2009). Both Ana3 and Sona are involved in cell survival and resistance to irradiation. Consistent with their positive genetic interaction and functional similarity, we found that Ana3 stabilizes Sona and increases the level of Sona in both wing discs and S2 cells. The truncated region in Ana3^{m19} protein is the most conserved region in Ana3/RTTN homologs, suggesting that this region plays a key role in stabilizing Sona. Some PMG mutations have also been identified in the Armadillo repeats in this carboxyl region of RTTN protein (Stouffs et al., 2018).

Both lethality and the small wing phenotype induced by Sona overexpression were completely rescued by knockdown of Ana3, suggesting that one of the main functions of Ana3 is to stabilize Sona (Fig. 3). It is worth noting that a degradation of Sona occurs in the lysosome but not in the proteasome complex, as well as that another *sona* suppressor Arr also stabilizes Sona (Han et al., 2020). Since our original genetic screen was aimed at identifying suppressors that reduce Sona activity, it makes sense that both *ana3* and *arr* mutants are identified as *sona* suppressors. Interestingly, Ana3 dramatically increased the level of exosomal Sona but not soluble Sona (Fig. 7). This suggests that Ana3 stabilizes Sona in the exosomal secretion pathway that is interconnected with the lysosomal degradation pathway and the endosomal pathway but not in Golgi transport (Repnik et al., 2013).

The loss of *ana3* induced cell death, which is a common phenotype of centrosome components (Fig. 4). Interestingly, overexpression of Ana3 enhanced the survival rate of irradiated flies, with wing discs showing the increased level of Ana3 1 h after irradiating the larvae, indicating that signals initiated by irradiation increase the level of Ana3 to prevent cell death. Since Ana3 stabilizes Sona, and knockdown of *ana3* completely rescues the lethality caused by overexpressed Sona, the ability of Ana3 in promoting cell survival may stem from stabilized Sona. We have previously shown that Sona-expressing cells are resistant to irradiation in a cell autonomous manner, and Sona secreted from these cells enables neighboring cells to survive and proliferate in a non-cell autonomous manner (Tsogtbaatar et al., 2019). Thus, it is possible that the increased level of Ana3 by irradiation contributes to increasing the level of Sona, which in turn functions to promote cell survival in both cell-autonomous and non-cell autonomous manners.

Extracellular Sona cleaves Wg and generates Wg-CTD that increases the level of Cyc D for initiating cell cycles (Won et al., 2019). Cyc D1 in mammalian cells promotes cell proliferation in response to mitogens, but overexpression of Cyc D1 leads to centrosome amplification, deregulation of the mitotic spindle, and chromosome abnormalities (Nelsen et

al., 2005). Cyc D1 is oncogenic in many human cancer cells because it contributes to malignant transformation, with centrosome amplification by *ras* oncogene depending on Cyc D1 (Zeng et al., 2011). The link between fly Cyc D, Sona, and Wg-CTD, as well as the association of many components in Wnt signaling such as Disheveled, Armadillo/β-catenin, Axin, and Arrow/LRP6 with centrosomes, suggests that Sona may participate in the regulation of centrosomal duplication for the initiation of cell cycles (Kaplan et al., 2004).

Note: Supplementary information is available on the Molecules and Cells website (www.molcells.org).

ACKNOWLEDGMENTS

We thank our lab members for critically reading this manuscript and giving valuable suggestions. We especially thank Dr. Jordan W. Raff for the generous offering of all fly lines, antibodies, and constructs. We also thank Bloomington Drosophila Stock Center, Drosophila Genetic Resource Center, and Developmental Studies Hybridoma Bank for fly strains and antibodies. This research was supported by the National Research Foundation of Korea (NRF) funded by the Ministry of Education, 2017R1A2B4009254 and 2019R1H1A2039726.

AUTHOR CONTRIBUTIONS

D.G.C., S.S.L., and K.O.C. designed the experiments and analyzed the data. D.G.C. and S.S.L. conducted the experiments. D.G.C. and K.O.C. wrote the paper.

CONFLICT OF INTEREST

The authors have no potential conflicts of interest to disclose.

ORCID

Dong-Gyu Cho https://orcid.org/0000-0003-2207-2163
Sang-Soo Lee https://orcid.org/0000-0001-9625-9276
Kyung-Ok Cho https://orcid.org/0000-0002-0760-2560

REFERENCES

Chen, P., Nordstrom, W., Gish, B., and Abrams, J.M. (1996). grim, a novel cell death gene in Drosophila. Genes Dev. *10*, 1773-1782.

Cho, K.O., Chern, J., Izaddoost, S., and Choi, K.W. (2000). Novel signaling from the peripodial membrane is essential for eye disc patterning in Drosophila. Cell *103*, 331-342.

Clevers, H. and Nusse, R. (2012). Wnt/beta-catenin signaling and disease. Cell *149*, 1192-1205.

Faisst, A.M., Alvarez-Bolado, G., Treichel, D., and Gruss, P. (2002). Rotatin is a novel gene required for axial rotation and left-right specification in mouse embryos. Mech. Dev. *113*, 15-28.

Gross, J.C., Chaudhary, V., Bartscherer, K., and Boutros, M. (2012). Active Wnt proteins are secreted on exosomes. Nat. Cell Biol. *14*, 1036-1045.

Gulsen, T., Hadjicosti, I., Li, Y., Zhang, X., Whitley, P.R., and Chalmers, A.D. (2016). Truncated RASSF7 promotes centrosomal defects and cell death. Dev. Biol. *409*, 502-517.

Han, J.H., Kim, Y., and Cho, K.O. (2020). Exosomal arrow (Arr)/lipoprotein receptor protein 6 (LRP6) in Drosophila melanogaster increases the extracellular level of Sol narae (Sona) in a Wnt-independent manner. Cell Death Dis. *11*, 944.

Jaklevic, B.R. and Su, T.T. (2004). Relative contribution of DNA repair, cell cycle checkpoints, and cell death to survival after DNA damage in Drosophila larvae. Curr. Biol. *14*, 23-32.

Kalimutho, M., Sinha, D., Jeffery, J., Nones, K., Srihari, S., Fernando, W.C., Duijf, P.H., Vennin, C., Raninga, P., Nanayakkara, D., et al. (2018). CEP55 is a determinant of cell fate during perturbed mitosis in breast cancer. EMBO Mol. Med. *10*, e8566.

Kaplan, D.D., Meigs, T.E., Kelly, P., and Casey, P.J. (2004). Identification of a role for beta-catenin in the establishment of a bipolar mitotic spindle. J. Biol. Chem. *279*, 10829-10832.

Karpen, G.H. and Schubiger, G. (1981). Extensive regulatory capabilities of a Drosophila imaginal disk blastema. Nature *294*, 744-747.

Katanayeva, N., Kopein, D., Portmann, R., Hess, D., and Katanaev, V.L. (2010). Competing activities of heterotrimeric G proteins in Drosophila wing maturation. PLoS One *5*, e12331.

Kelwick, R., Desanlis, I., Wheeler, G.N., and Edwards, D.R. (2015). The ADAMTS (A Disintegrin and Metalloproteinase with Thrombospondin motifs) family. Genome Biol. *16*, 113.

Kheradmand Kia, S., Verbeek, E., Engelen, E., Schot, R., Poot, R.A., de Coo, I.F., Lequin, M.H., Poulton, C.J., Pourfarzad, F., Grosveld, F.G., et al. (2012). RTTN mutations link primary cilia function to organization of the human cerebral cortex. Am. J. Hum. Genet. *91*, 533-540.

Kim, G.W., Won, J.H., Lee, O.K., Lee, S.S., Han, J.H., Tsogtbaatar, O., Nam, S., Kim, Y., and Cho, K.O. (2016). Sol narae (Sona) is a Drosophila ADAMTS involved in Wg signaling. Sci. Rep. *6*, 31863.

Kim, Y. and Cho, K.O. (2020). POU domain motif3 (Pdm3) induces wingless (wg) transcription and is essential for development of larval neuromuscular junctions in Drosophila. Sci. Rep. *10*, 517.

Logan, C.Y. and Nusse, R. (2004). The Wnt signaling pathway in development and disease. Annu. Rev. Cell Dev. Biol. *20*, 781-810.

McLean, I.W. and Nakane, P.K. (1974). Periodate-lysine-paraformaldehyde fixative. A new fixative for immunoelectron microscopy. J. Histochem. Cytochem. *22*, 1077-1083.

Nam, S. and Cho, K.O. (2020). Wingless and Archipelago, a fly E3 ubiquitin ligase and a homolog of human tumor suppressor FBW7, show an antagonistic relationship in wing development. BMC Dev. Biol. *20*, 14.

Nelsen, C.J., Kuriyama, R., Hirsch, B., Negron, V.C., Lingle, W.L., Goggin, M.M., Stanley, M.W., and Albrecht, J.H. (2005). Short term cyclin D1 overexpression induces centrosome amplification, mitotic spindle abnormalities, and aneuploidy. J. Biol. Chem. *280*, 768-776.

Nguyen, D., Fayol, O., Buisine, N., Lecorre, P., and Uguen, P. (2016). Functional interaction between HEXIM and Hedgehog signaling during Drosophila wing development. PLoS One *11*, e0155438.

Raslan, A.A. and Yoon, J.K. (2020). WNT signaling in lung repair and regeneration. Mol. Cells *43*, 774-783.

Repnik, U., Cesen, M.H., and Turk, B. (2013). The endolysosomal system in cell death and survival. Cold Spring Harb. Perspect. Biol. *5*, a008755.

Song, D.H., Dominguez, I., Mizuno, J., Kaut, M., Mohr, S.C., and Seldin, D.C. (2003). CK2 phosphorylation of the armadillo repeat region of beta-catenin potentiates Wnt signaling. J. Biol. Chem. *278*, 24018-24025.

Stevens, N.R., Dobbelaere, J., Wainman, A., Gergely, F., and Raff, J.W. (2009). Ana3 is a conserved protein required for the structural integrity of centrioles and basal bodies. J. Cell Biol. *187*, 355-363.

Stouffs, K., Moortgat, S., Vanderhasselt, T., Vandervore, L., Dica, A., Mathot, M., Keymolen, K., Seneca, S., Gheldof, A., De Meirleir, L., et al. (2018). Biallelic mutations in RTTN are associated with microcephaly, short stature and a wide range of brain malformations. Eur. J. Med. Genet. *61*, 733-737.

Strigini, M. and Cohen, S.M. (2000). Wingless gradient formation in the Drosophila wing. Curr. Biol. *10*, 293-300.

Torres, J.Z., Summers, M.K., Peterson, D., Brauer, M.J., Lee, J., Senese, S.,

Gholkar, A.A., Lo, Y.C., Lei, X., Jung, K., et al. (2011). The STARD9/Kif16a kinesin associates with mitotic microtubules and regulates spindle pole assembly. Cell *147*, 1309-1323.

Tsogtbaatar, O., Won, J.H., Kim, G.W., Han, J.H., Bae, Y.K., and Cho, K.O. (2019). An ADAMTS Sol narae is required for cell survival in Drosophila. Sci. Rep. *9*, 1270.

Vakifahmetoglu, H., Olsson, M., and Zhivotovsky, B. (2008). Death through a tragedy: mitotic catastrophe. Cell Death Differ. *15*, 1153-1162.

Vandervore, L.V., Schot, R., Kasteleijn, E., Oegema, R., Stouffs, K., Gheldof, A., Grochowska, M.M., van der Sterre, M.L.T., van Unen, L.M.A., Wilke, M., et al. (2019). Heterogeneous clinical phenotypes and cerebral malformations reflected by rotatin cellular dynamics. Brain *142*, 867-884.

Won, J.H., Kim, G.W., Kim, J.Y., Cho, D.G., Kwon, B., Bae, Y.K., and Cho, K.O. (2019). ADAMTS Sol narae cleaves extracellular Wingless to generate a novel active form that regulates cell proliferation in Drosophila. Cell Death Dis. *10*, 564.

Zeng, D.X., Xu, Y.J., Liu, X.S., Wang, R., and Xiang, M. (2011). Cigarette smoke extract induced rat pulmonary artery smooth muscle cells proliferation via PKCalpha-mediated cyclin D1 expression. J. Cell. Biochem. *112*, 2082-2088.